Asia-Pacific Journal of Science and Technology: Volume: 25. Issue: 04. Article ID.: APST-25-04-04. Research Article

APST

Asia-Pacific Journal of Science and Technology

https://www.tci-thaijo.org/index.php/APST/index

Published by the Research and Graduate Studies,
Khon Kaen University, Thailand

A DFT study of C, SiC, Si, and SiGe colloidal quantum dots for bioimaging

Ruhan Thirayatorn[1], Pornsawan Sikam[5], Pairot Moontragoon[1,2,3,*] and Zoran Ikonic[4]

[1]Department of Physics, Khon Kaen University, Khon Kaen, Thailand
[2]Institute of Nanomaterials Research and Innovation for Energy (IN-RIE), NANOTEC-KKU RNN on Nanomaterials Research and Innovation for Energy, Khon Kaen University, Khon Kaen, Thailand
[3]Thailand Center of Excellence in Physics, Commission on Higher Education, Bangkok, Thailand
[4]School of Electronic and Electrical Engineering, University of Leeds, Leeds, United Kingdom
[5]NANOTEC, National Science and Technology Development Agency (NSTDA),Pathum Thani, Thailand
[*]Corresponding author: mpairo@kku.ac.th

Received 7 June 2020
Revised 20 October 2020
Accepted 21 October 2020

Abstract

Photoluminescence of colloidal nanocrystals or quantum dots has great potential in bioanalysis and diagnostic applications, as well as in optoelectronics. In this work C, SiC, Si, and SiGe colloidal quantum dots are formed based on the diamond structure or zinc blende structure with various diameters. Then, an energy-optimized structure was developed, and the electronic structure was investigated using density functional theory (DFT). The absorption coefficient of the energy spectrum of these dots is studied by employing a time-dependent density functional theory (TD-DFT) method. The calculated geometries indicated that these dots are nearly spherical. The electronic structure reveals that the highest occupied molecular orbital (HOMO) and the lowest unoccupied molecular orbital (LUMO) of energy level can be tuned by changing the quantum dot size, i.e., the energy gaps are reduced when the diameter of these dots is increased. The studied absorption energy reveals that the absorption peak is in the UV-vis range. Moreover, the absorption peak can be engineered, i.e., the absorption wavelength position is blueshifted when the size of the quantum dot is increased, both in the same materials, but in different forms and in the same form of different materials.

Keywords: C colloidal quantum dots, Si colloidal quantum dots, SiC colloidal quantum dots, SiGe colloidal quantum dots

1. Introduction

Nanotechnology is important in daily life. There are extensive research studies with industrial applications. The structure of these materials is nanoscale or about 1-100 nanometers in size. Their optical, electrical, magnetic, and mechanic properties are different although they are made of the same materials [1-3]. Quantum dots, called “artificial atoms”, are one type of nanomaterials. Researchers have developed these materials with suitable properties for applications such as drug delivery, bio-sensing, bio-imaging, medical biology, lasers, optoelectronics and photoluminescence. In recent years, several methods have been developed for synthesis of quantum dots including arc discharge, laser ablation, electrochemical oxidation, microwave irradiation, and hydrothermal methods [1-8]. When applied for medical applications in the human body, toxicity is a primary consideration. CdTe, CdAs, PbS are highly fluorescent but damage cells. So, researchers seek to develop new quantum dots that are strongly luminescent with low toxicity. Carbon and silicon quantum dots are currently very attractive. They have been widely researched for solar cell applications. Generally, the optical properties of these quantum dots depend on the size of their component particles and their terminal surface functional groups [9-14]. The aim of this work was too fabricate spherical C-dots, Si-dots, SiC-dots, and SiGe-dots and arrange their atoms based on a diamond structure. We calculated the absorption energy of the optimized structure and compared the effects of nanoparticle size and the type of dots.

2. Materials and methods

This paper reports a study of the optical properties of quantum dots. We define the structure of C, SiC, Si, and SiGe nanodots modeled on diamond or zinc blende structures. The shape of the dots is spherical with diameters in the range of 0.5-10 nm. We can reference the materials as dot2, dot3, and dot4. Each dot-type is a structured form with an integer representing the number of atoms comprising the structure. All these atoms are located within an initial radius before calculation. Bonding is absent at the surface atom of the dots, so we terminated the surface sites with hydrogen atoms to fill the bonding sites. Figure 1 shows the structures used in this calculation. All calculations in this work are based on density functional theory (DFT) employing a hybrid functional (B3LYP) with a 6-31g basis set. All energies were obtained using geometries optimized with SCC-DFTB. The electronic absorption energy was also investigated with time-dependent density functional theory employing a hybrid functional (B3LYP) and 6-31g basis set using the obtained energy optimization structures. All calculations were performed with the Gaussain09 package [15].

3. Results and discussion

3.1 The energy-optimized structure

The optimized C, SiC, Si, and SiGe nanostructures are shown in Figure 2 with various diameters and materials. C, Si, SiC, and SiGe are used in the current this work. The position of atoms changes when the structures were calculated at the ground state. The quantum dots are nearly spherical and they remain as diamond structures, especially for the large dots, i.e., dot3 and dot4. However, for the smaller dot (dot2), the optimized quantum dot forms are likely plane cluster structures because of the fewer number of the atoms in the quantum dots. The bond lengths are calculated and shown in Table 1. The bond length values are close to those of other calculations [16], with experiment results of 1.54 A˚ for C–C, 1.12 A˚ for C–H [17-18], and about 2.36 A˚ for Si–Si bond lengths in sila-adamantane [19]. The Ge–H and Ge–Ge bond lengths are also in good agreement with previously published results [20-21]. The bond angles of the structures detected are presented in Table 2. It was found that the bond angle of the pure C-dots and Si-dots is around 109˚, which is close to that of the diamond structure. This occurs since the SiC-dots and SiGe-dot are comprised of two atoms. Therefore, there is a different value from that of the standard tetrahedral structure. The diameters, HOMO and LUMO energy levels, as well as the HOMO-LUMO gaps of all quantum dots are presented in Table 3. The diameters were sorted in ascending order for the same structural form as C-dots < SiC-dot < Si-dot < SiGe-dots. This occurs because the radius of a C atom is less than Si, Ge atoms. However, the diameters of the Si-dots are slightly larger than those of SiGe-dots in the cases of dot3 and dot4. This is because the total number of atoms in the SiGe dots is slightly greater than that in the Si dots. The energy gaps are determined by the energy level difference between the HOMO and LUMO levels. The trend of the HOMO-LUMO energy level is reducing when the size of the nanodot is expanded for all C, SiC, Si, and SiGe-dots. This is a direct impact of the quantum size effect. Although it is the same material, it has a different size. A smaller structure has a wider gap than a larger one.

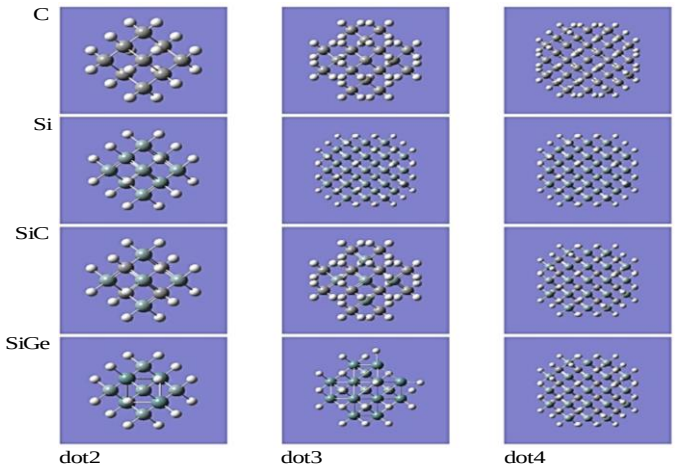

Figure 1 The structure of C, Si, SiC, SiGe -dots before optimization.

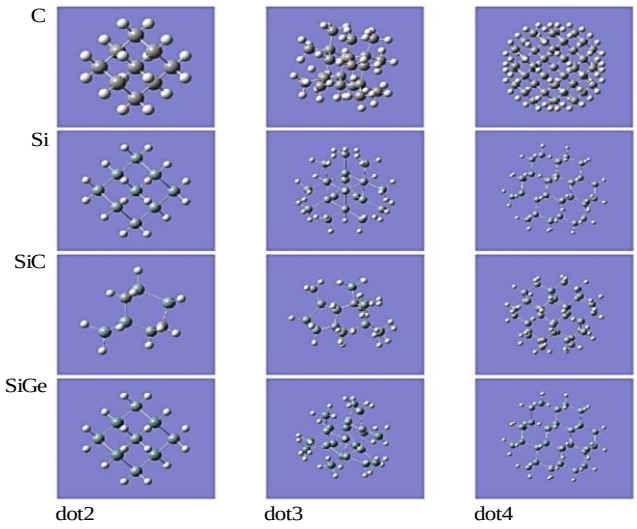

Figure 2 The structure of C, Si, SiC, SiGe-dots after optimization by DFT with B3LYP/6-31g.

Table 1 The bond angles of the quantum dots.

Silicon carbide	Quantum dots	Bond Angle			
C		C-C-C			
	dot2	109.54			
	dot3	110.78			
	dot4	109.81			
Si		Si-Si-Si			
	dot2	109.20			
	dot3	109.68			
	dot4	109.29			
SiC		C-Si-C	C-C-C	Si-Si-Si	Si-C-Si
	dot2	108.00	114.84	92.85	113.35
	dot3	115.88	113.36	100.05	105.98
	dot4	110.64	109.74	100.81	105.43
SiGe		Si-Ge-Si		Ge-Si-Ge	
	dot2	109.49		109.45	
	dot3	108.82		109.31	
	dot4	108.88		108.54	

Table 2 The bond lengths of quantum dots.

Silicon carbide	Quantum dots	Diameter (Å)	C-C (Å)	C-H (Å)			
C	dot2	4.781	1.544	1.099			
	dot3	7.535	1.588	1.090			
	dot4	9.457	1.566	1.093			
			1.543	1.100			
Other calculations			1.54	1.12			
experimental			ref. [17-18]	ref. [17-18]			
Si			Si-Si (Å)	Si-H (Å)			
	dot2	7.354	2.364	1.494			
	dot3	11.199	2.372	1.489			
	dot4	14.5	2.383	1.491			
			2.373	1.498			
Other calculations			2.36	1.480			
experimental			ref. [19]	(for SiH_4 ref. [22])			
SiC			Si-C (Å)	C-C (Å)	Si-Si (Å)	Si-H (Å)	C-H (Å)
	dot2	6.184	1.914	1.558	2.345	1.494	1.100
	dot3	9.552	1.927	1.586	2.367	1.491	1.095
	dot4	12.174	1.936	1.589	2.303	1.492	1.097
			1.86	1.543	2.373	1.480	1.100
Other calculations				1.54	2.36	1.480	1.12
experimental				ref. [17-18]	ref. [19]	(for SiH_4 ref. [22])	ref. [17-18]
SiGe			Si-H (Å)	Ge-H (Å)	Si-Ge (Å)		
	dot2	7.445	1.503	1.544	2.396		
	dot3	10.94	1.513	1.535	2.365		
	dot4	14.376	1.527	1.542	2.438		
			1.48	1.587	2.388		
Other calculations			1.480		2.364		
experimental			(for SiH_4 ref. [22])		(ref. [23])		

Table 3. The diameter of optimized dots as well as HOMO and LUMO energy levels and the HOMO-LUMO gap.

Silicon carbide	Quantum dots	Diameter (Å)	HOMO (eV)	LUMO (eV)	HOMO – LUMO (eV)	Other calculations (eV)
C	dot2	4.781	-7.442	1.886	9.328	9.32 (ref. [16])
	dot3	7.535	-7.166	1.977	9.143	
	dot4	9.457	-5.878	1.713	7.592	
Si	dot2	7.354	-7.503	-0.627	6.876	6.87 (ref. [16])
	dot3	11.199	-6.230	-1.523	4.707	
	dot4	14.500	-6.329	-2.024	4.305	
SiC	dot2	6.184	-6.766	0.160	6.926	6.4 (ref. [24])
	dot3	9.552	-6.463	-0.999	5.464	
	dot4	12.174	-5.314	-0.749	4.565	
SiGe	dot2	7.445	-7.398	-0.492	6.905	
	dot3	10.940	-6.147	-1.276	4.871	4.39 (ref. [25])
	dot4	14.376	-6.213	-1.727	4.487	

3.2 Electron affinity (EA)

The adiabatic electron affinity (AEA) is defined as AEA = $E^{neutral}$ - E^{anion}, where $E^{neutral}$ is the total energy of the neutral molecule at its optimized geometry, whereas E^{anion} is the total energy of the corresponding anion calculated at its optimized geometry. In Table 2 and Figure 3, the HOMO and LUMO states are calculated using DFT with the B3LYP/6-31g basis set and Koopmans' theorem [26], i.e., the first ionization energy of a molecular system is equal to the negative value of the orbital energy of the highest occupied molecular orbital (HOMO). Electron affinity is equal to the negative value of lowest unoccupied molecular orbital (LUMO). The electron affinity energy (EA) of the colloidal quantum dot is tunable, i.e., it is diminished when the radius of the nanodot is increased. The carbon and SiC (dot2) nanodots show especially high negative electron affinity (NEA) because the LUMO state energy is in the positive energy region. Therefore, these structures could have the potential for innovative applications, such as advanced photoemission devices, advanced secondary electron emission devices, field electron emission devices, thermionic emission devices, and cold cathode applications.

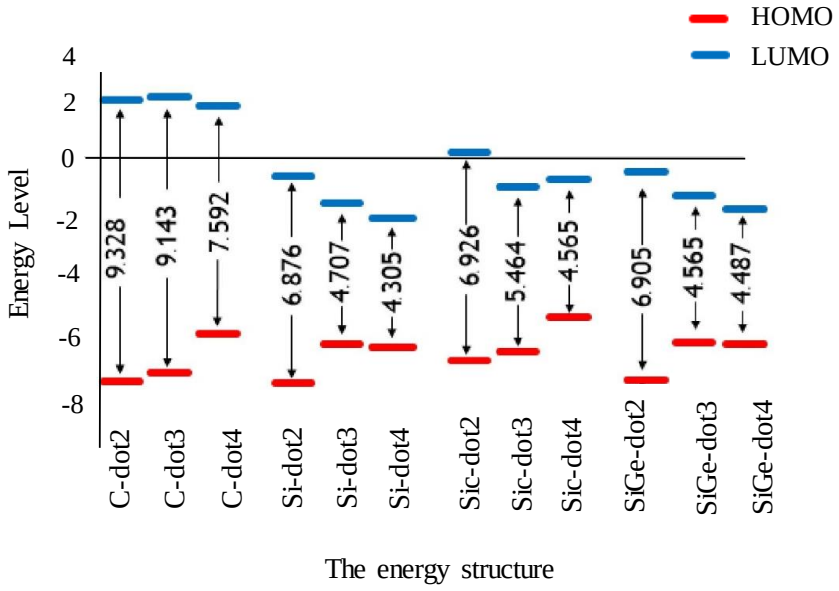

Figure 3 The energy gap (eV) between the HOMO – LUMO level.

3.3 The molecular orbital distribution

Corresponding to the energy-optimized wave function, the highest occupied molecular orbital (HOMO) and the lowest unoccupied molecular orbital (LUMO) tend to be localized around the quantum dot surface. The energy gap between the HOMO and LUMO states is size-dependent. The value of the energy gap decreases as the dot size increases, as shown in our results (Table 3). It also indicates that confinement states are weaker for larger dot sizes. However, this work focused on only the difference between the location of the distribution of HOMO and LUMO. According to Figure 4, there is a slight difference in the location of the distribution of HOMO and LUMO states in all dot sizes. Therefore, electrons in the colloidal quantum dots are easily transferred from the HOMO to the LUMO state.

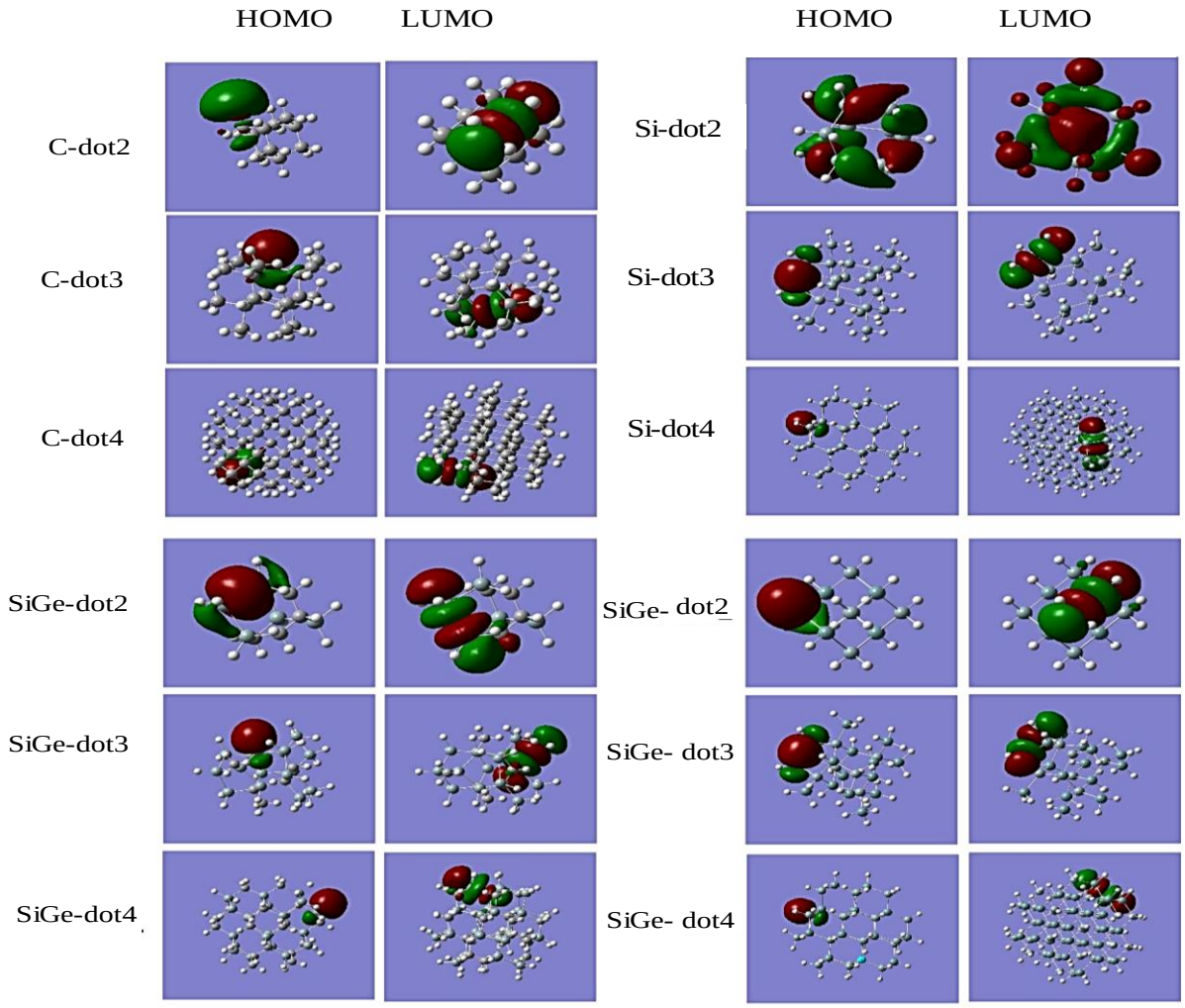

Figure 4 Molecular orbital spatial distribution of hydrogen-capped colloidal carbon, silicon, SiC, and SiGe quantum dots with sizes of dot2, dot3, dot4, respectively.

3.4 The electronic absorption spectra

Simulation of the absorption spectra of the dots is a preliminary evaluation of light-harvesting ability, which has medical and bio-sensing applications based their energy absorption. The calculated wavelengths and oscillator strengths of the quantum dots in a vacuum are obtained through TD-DFT calculations with a hybrid functional (B3LYP) and a 6-31g basis using the Gaussain09 software package [15].

The simulated absorption spectra of these dots are shown in Figure 5 for the C-dot (a), Si-dot (b), SiC (c) and SiGe (d). The absorption peaks of the C-dot are at wavelengths of 146.8 nm, 147.9 nm, and 177.4 nm for dot2 (0.47 nm), dot3 (0.75 nm), and dot4 (0.95 nm), respectively. This confirms that the absorption spectrum is tunable by changing the cluster size. It reasonably agrees with the experiment results of Miao et al. [27]. Carbon-dots with average particle sizes of 3.96 nm, 4.12 nm, and 4.34 nm have absorption wavelengths of 440 nm, 540 nm, and 620 nm, respectively, for the blue, green, and red spectra. In the case of Si-dots, the absorption

energies are 212.0 nm (dot2), 317.4 nm (dot3), and 334.2 nm (dot4). These results are comparable to colloidal silicon nanocrystals as the mean size decreases from 4.23 to 1.42 nm, which have blue emissions peaks at 405 and 430 nm, prepared using a laser ablation method [28]. There are three SiC absorption peaks at wavelengths of 205.9 nm (dot2), 258.1 nm (dot3), and 306.5 nm (dot4). In the case of SiGe, we also found three absorption peaks at 212 nm (dot3), 297 nm (dot3), and 312.2 nm (dot4). These electronic absorption peaks, in all cases, were in the UV-vis range. Summarizing these results, the size of quantum dots is considered the most influential parameter since the structures are the same among the materials. The position of peak absorption energy will increase with the diameter of the quantum dots. From Figure 6, comparing various materials in the dot4 form, the lowest to highest peak absorption energies are for the C-dot, SiC-dot, SiGe-dot, respectively. The important effect for this point is due to the quantum sized nanoparticles. The Si-dot has the largest diameter and it has a peak absorption in the highest position in nm units. When pure Si-dots are substituted with C atoms in their structure, the energy gap of the pure Si-dots is larger than that of the pure C dots. The peak absorption of SiC will be located at a position intermediate between the pure Si-dots and C-dots.

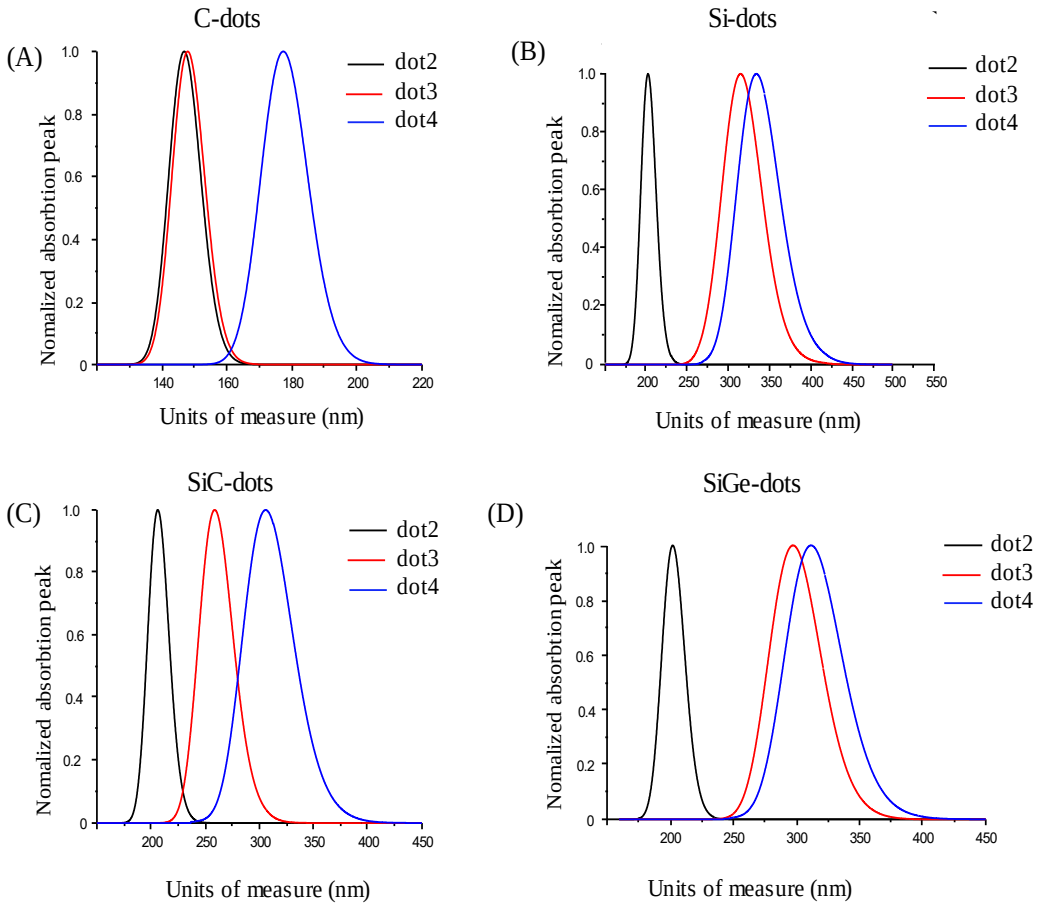

Figure 5 Energy absorption peaks of C-dots (A), Si-dots (B), SiC-dots (C) and SiGe-dots (D).

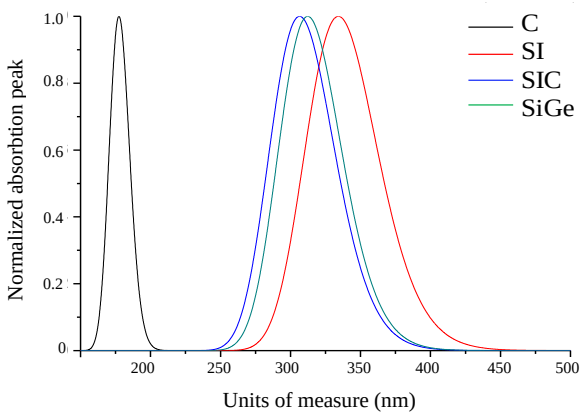

Figure 6 Comparison of the energy peak absorption values of dot4 comprised of C, Si, SiC, and SiGe – dots.

4. Conclusion

In this work, we propose C, SiC, Si, and SiGe quantum dots as potential materials for use in biomarker- and bioimaging-related applications. The geometries and electronic properties of the C, SiC, Si, and SiGe quantum dots were studied using a DFT method. UV-vis absorption was investigated using a TD-DFT method. The dots were spherical and based on the diamond structure. The HOMO-LUMO gap decreases when the radius of the nanodots increases. Considering the size of the quantum dot at the ground state using various materials with the same number of atoms, the increased diameter of the dots is caused by the presence of larger atoms. The calculated electronic absorption energy of these quantum dots was found to be in the UV-vis range. The position of absorption tended to increase with the diameter of the dots in the same material, as well as in the different forms as well as in the same form (dot4) in different materials. Properties of the dots are tunable by changing the dot size, doping, or substitution of other atoms into a pure structure, so that they can be made suitable for many applications.

5. Acknowledgments

This work has received scholarship under the Post-Doctoral Training Program from Khon Kaen University, Thailand, the Research Network NANOTEC (RNN) program of the National Nanotechnology Center (NANOTEC), NSTDA, Ministry of Higher Education, Science, Research and Innovation and Khon Kaen University, Thailand, National Research Council of Thailand (NRCT).

6. References

[1] Mao XJ, Zheng HZ, Long YJ, Du J, Hao JY, Wang LL, et al. Study on the fluorescence characteristics of carbon dots. Spectrochim Acta Part A. 2010;75:553-557.

[2] Li QL, Yuan FL, Lei Z, Yue L, Cheng ZH. One-step synthesis of fluorescent hydroxyls-coated carbon dots with hydrothermal reaction and its application to optical sensing of metal ions. Sci China Chem. 2011;54:1342-1347.

[3] Hu L, Sun Y, Li S, Wang X, Wang LX, Wu Y. Multifunctional carbon dots with the high quantum yield for imaging and gene delivery. Carbon. 2013;67:508-513.

[4] Sun YP, Zhou B, Lin Y, Wang W, Fernando KAS, Pathak P, et al. Quantum-sized carbon dots for bright and colorful photoluminescence. J Am Chem Soc. 2006;128(24):7756-7757.

[5] Dong Y, Zhou N, Lin X, Lin J, Chi Y, Chen G. Extraction of electrochemiluminescent oxidized carbon quantum dots from activated carbon. Chem Matter. 2010;22(21):5895-5899.

[6] Dong Y, Wang R, Li H, Shao J, Chi Y, Lin X, et al. Polyamine-functionalized carbon quantum dots as fluorescent probes for selective and sensitive detection of copper ions. Anal Chem. 2012;84(14):6220-6224.

[7] Sun YP, Wang X, Lu F, Cao L, Meziani MJ, Luo PG, et al. Doped carbon nanoparticles as a new platform for highly photoluminescent dots. J Phys Chem C. 2008;112(47):18295-18298.

[8] Zhu J, Booker C, Li R, Zhou X, Sham TK, Sun X, et al. An electrochemical avenue to blue luminescent nanocrystals from multiwalled carbon nanotubes (MWCNTs). J Am Chem Soc. 2007;129(4):744-745.

[9] Wang Q, Zhang H, Long Y, Zhang L, Gao M, Bai W. Microwave–hydrothermal synthesis of fluorescent carbon dots from graphite oxide. Carbon. 2011;49(9):3134-3140.

[10] Shiohara A, Hanada S, Prabaker S, Fujioka K, Lim TH, Yamamoto K, et al. Chemical reactions on surface molecular attached to silicon quantum dot. J Am Chem Soc. 2010;132(1):248-253.
[11] Zhao S, Liu X, Pi X, Yang D. Light-emitting diodes based on colloidal silicon quantum dots. J Semicon. 2018;39(6):061008.
[12] Reboredo FA, Pizzagalli L, Galli G. Computational engineering of the stability and optical gaps of SiC quantum dots. Nano Letters. 2004;4(5):801-804.
[13] Wu XK, Chenb WJ, Yu YS, Tang YL. The first principle study of the electronic structure of SixGe (1−x) alloy films. Phys Lett A. 2018;382(47):3418-3422.
[14] Frisch MJ, Trucks GW, Schlegel HB, Scuseria GE, Robb MA, Cheeseman JR, et al. Gaussian 09, revision A.1, Gaussian, Inc.. Wallingford CT. 2009.
[15] Marsusi F, Mirabbaszadeh K, Mansoori GA. Opto-electronic properties of adamantane and hydrogen-terminated sila-and germa-adamantane: a comparative study. Physica E Low Dimens Syst Nanostruct. 2009;41(7):1151-1156.
[16] Nowacki W, Hedberg KW. An electron diffraction investigation of the structure of adamantane. J Am Chem Soc. 1948;70:1497-1500.
[17] Amoureux JP, Foulon M. Comparison between structural analyses of plastic and brittle crystals. Acta Crystallogr Sect B Struct Sci. 1987;43:470-479.
[18] Fischer J, Baumgartner J, Marschner C. Synthesis and structure of sila adamantane. Science. 2005;310: 825.
[19] Dyall K, Taylor P, Faegri K, Partridge H. All-electron molecular dirac-hartree-fock calculations: the group IV tetrahydrides CH_4, SiH_4, GeH_4, SnH_4, and PbH_4. J Chem Phys. 1991;95:2583.
[20] Beagley B, Monaghan JJ. Electron diffraction study of digermane. Trans Faraday Soc. 1970;66:2745.
[21] Boyd DRJ. Infrared spectrum of trideuterosilane and the structure of the silane molecule. J Chem Phys. 1955;23(5):922.
[22] Hinchley SL, McLachlan LJ, Robertson HE, Rankin DWH, Seppälä E. Wolf-walther du mont, steric and electronic effects on Si–Ge bond lengths: an experimental and theoretical structural study of Me2Ge(SiCl3)2 and Me3GeSiCl3. Inorganica Chim Acta. 2007;360(4):1323-1331.
[23] Saha S, Sarkar P. Tuning the HOMO–LUMO gap of SiC quantum dots by surface functionalization. Chem Phys Lett. 2012;536:118-122.
[24] Niaz S, Zdetsis AD, Badar MA, Hussain S, Sadiq I, Khan MA, et al. Optical properties of pure and mixed germanium and silicon quantum dots. J Chem Soc Pak 2016;38(02):211
[25] Heinrich N, Koch W, Frenking G. On the use of Koopmans' theorem to estimate negative electron affinities. Chem Phys Lett. 1986;124(1):20-25.
[26] Miao X, Qu D, Yang D, Nie B, Zhao Y, Fan H, et al. Synthesis of carbon dots with multiple color emission by controlled graphitization and surface functionalization. Adv Mater. 2018;30:1704740.
[27] Zhang YX, Wu WS, Hao HL, Shen WZ. Femtosecond laser-induced size reduction and emission quantum yield enhancement of colloidal silicon nanocrystals: effect of laser ablation time. Nanotechnology. 2018;29(36):365706.